

# Dayside ionospheric plasma convection, electric fields, and field-aligned currents derived from the SuperDARN radar observations and predicted by the IZMEM model

A. V. Kustov,<sup>1</sup> V. O. Papitashvili,<sup>2</sup> G. J. Sofko,<sup>1</sup> A. Schiffer,<sup>1</sup>  
 Y. I. Feldstein,<sup>3</sup> L. I. Gromova,<sup>3</sup> A. E. Levitin,<sup>3</sup> B. A. Belov,<sup>3</sup>  
 R. A. Greenwald,<sup>4</sup> and M. J. Ruohoniemi<sup>4</sup>

**Abstract.** A recent deployment of the Super Dual Auroral Radar Network (SuperDARN) HF radar network provides excellent opportunities to construct two-dimensional maps of the ionospheric convection over large areas in both the northern and southern polar regions. The Institute of Terrestrial Magnetism, Ionosphere and Radiowave Propagation electrodynamic model (IZMEM) is a potentially useful tool for predicting, also on a global scale, the ionospheric plasma convection patterns, electric fields, magnetic disturbances, ionospheric and field-aligned currents. Comparisons of the IZMEM predictions with satellite and incoherent scatter radar data show that the model's performance is reasonably good, but the model needs more extensive and accurate verifications. In this paper, several events under relatively stable IMF conditions ( $B_z < 0$  and  $B_z > 0$ ) are studied and discussed. The SuperDARN/IZMEM ion drift velocities are found to be in reasonable agreement in both magnitude and direction; the average difference (over the individual SuperDARN convection map) between the predicted magnitude of the ion drift velocity and the measured magnitude is about 50%, while the difference in the direction is typically less than 25°. The IZMEM predictions of the location, direction, and magnitude of field-aligned currents also agree well with the SuperDARN observations. It is concluded that simultaneous use of SuperDARN data and IZMEM model can improve the specification of the polar ionospheric convection for space weather applications.

## 1. Introduction

Numerous measurements obtained from a variety of ground-based platforms and satellite instruments show a strong relationship between the solar wind state near the Earth's orbit and the plasma convection in the magnetosphere and therefore in the ionosphere [e.g., Kamide and Baumjohann, 1993]. These observations have led to a number of studies which elucidate the electrodynamic coupling between the magnetosphere and ionosphere as well as provide better opportunities for specification and forecasting of space weather in the near-Earth's environment. As mentioned by Maynard

[1995], the studies of ionospheric convection and distribution of field-aligned currents are essential components of the U. S. National Space Weather Initiative.

Despite the fact that a number of ionospheric convection models, based on satellite, radar, and ground magnetometer data, have already been developed [e.g., Levitin *et al.*, 1982; Foster, 1983; Feldstein and Levitin, 1986; Heppner and Maynard, 1987; Hairston and Heelis, 1990; Papitashvili *et al.*, 1994; Rich and Hairston, 1994; Weimer, 1995, 1996; Ruohoniemi and Greenwald, 1996], the complexity of relationships between the plasma convection and changing interplanetary conditions requires further studies and intercalibration between the multi-instrument measurements and different modeling techniques. In other words, the experimentally verified model of the ionospheric convection parameterized by the interplanetary magnetic field (IMF) strength and direction and the solar wind conditions is required for practical applications.

In recent years, with the almost completed deployment of the Super Dual Auroral Radar Network (SuperDARN), the opportunities for detailed studies of high-latitude ionospheric convection are significantly increased [Greenwald *et al.*, 1995a]. In the northern hemisphere, the SuperDARN network covers a substantial

<sup>1</sup>Institute of Space and Atmospheric Studies, University of Saskatchewan, Saskatoon, Saskatchewan, Canada.

<sup>2</sup>Space Physics Research Laboratory, University of Michigan, Ann Arbor.

<sup>3</sup>Institute of Terrestrial Magnetism, Ionosphere, and Radio Wave Propagation, Troitsk, Russia.

<sup>4</sup>Applied Physics Laboratory, Johns Hopkins University, Laurel, Maryland.

part of the high-latitude ionosphere ( $\sim 15$  hours of local time) and provides measurements of the plasma drifts with a time resolution of several minutes. SuperDARN operates now on a continuous basis; information about radars and data availability can be obtained via the World Wide Web (<http://sd-www.jhuapl.edu/RADAR>). Therefore the SuperDARN data can easily be compared with measurements made by other ground-based or satellite instruments or incorporated into any modeling technique for space weather forecasting purposes.

A new statistical model of the ionospheric convection binned by the IMF strength and direction was recently developed at Johns Hopkins University, Applied Physics Laboratory (JHU/APL) [Ruohoniemi and Greenwald, 1996]. This model utilizes the SuperDARN data obtained from the Goose Bay HF radar by fitting the data with a combination of harmonic functions whose coefficients satisfy requirements of a minimum least error. (This approach was suggested and utilized first by Weimer [1995, 1996] for the DE 2 satellite electric field measurements.) Thus for known IMF parameters, the electrostatic potential distributions can now be predicted from the JHU/APL model with the reasonable accuracy within the range of available experimental data. The quality of predictions by this model for arbitrary solar wind and IMF conditions needs to be investigated further.

The large-scale patterns of the ionospheric plasma convection at high latitudes have been obtained from ground magnetometer data and extensively analyzed analytically as well as numerically in numerous studies [e.g., Kamide et al., 1981; Levitin et al., 1982; Friis-Christensen et al., 1985; Feldstein and Levitin, 1986; Richmond and Kamide, 1988; Papitashvili et al., 1990]. As a result, such practical techniques as the assimilative mapping of ionospheric electrodynamics (AMIE) [Richmond, 1992] and the Institute Terrestrial Magnetism, Ionosphere and Radiowave Propagation electrodynamic model (IZMEM) [Papitashvili et al., 1994] began to be widely used for a variety of scientific applications [e.g., Knipp et al., 1993; Papitashvili et al., 1995; Feldstein et al., 1996]. Both techniques are able to calculate the same set of ionospheric electrodynamic parameters (electric potential, magnetic and electric fields, ionospheric and field-aligned currents, and Joule heating rate) over both the northern and southern polar regions.

A chief advantage of these numerical methods is their ability to provide global coverage and reasonable time resolution for the events under study. The AMIE technique utilizes localized radar and/or satellite electric field measurements, but it also requires a collection of global magnetometer data for the event under study. The IZMEM technique is based on a regression analysis between IMF and ground magnetic variations (the "black box" approach, see details given by Papitashvili et al. [1994]); therefore it requires only the IMF data (strength and direction) for prediction of the ionospheric electrodynamic parameters. The IZMEM model is also

accessible via the World Wide Web (<http://www.sprl.umich.edu/MIST>).

The IZMEM model has been constructed from the hourly mean IMF and ground geomagnetic field values. Such averaging of experimental data helps to avoid uncertainties in the time delay between the IMF changes measured by a spacecraft and the corresponding ionospheric convection responses. The model's spatial resolution is about  $1^\circ$  in invariant (corrected geomagnetic) latitude ( $\Phi \geq 57^\circ$ ) and 1 hour in magnetic local time (MLT) (i.e.,  $15^\circ$  by the longitude). IZMEM utilizes a statistical model of ionospheric conductivity caused by both the particle precipitation [Wallis and Budzinski, 1981] and the photoionization.

Despite the fact that hourly averages have been used for the model's construction, a "black box" nature of the utilized regression approach (the IMF changes are used as the input; the ground geomagnetic responses are used as the output) allows us to apply the IZMEM model for studies of time-varying phenomena on a timescale up to 5-10 min resolution [e.g., Papitashvili et al., 1995; A. J. Ridley and V. O. Papitashvili, Dynamics of the ionospheric convection patterns during changes in the northward interplanetary magnetic field: A comparison between AMIE and IZMEM techniques, submitted to *Journal of Geophysical Research*, 1997, hereinafter referred to as submitted manuscript, 1997]. Thus the model itself is not the "hourly averaged" model but rather the dynamical, noninertial statistical model which shows the ground geomagnetic responses on any changes in the IMF. Note that one must be careful properly calculating the solar wind propagation time delay and selecting appropriate IMF values for the modeling.

Several studies have been undertaken to assess the accuracy of IZMEM modeling for space weather predictions [Feldstein et al., 1994, 1996; Papitashvili et al., 1995; Papitashvili and Papitashvili, 1996; Ridley and Papitashvili, submitted manuscript, 1997]. However, the results of comparisons with experimental measurements (e.g., satellite and/or radar data) are still controversial to some extent. On the one hand, during the quasi-steady IMF conditions, the IZMEM model shows realistic large-scale convection patterns determined by the global electric field distributions related to each IMF component [e.g., Feldstein and Levitin, 1986; Papitashvili et al., 1994]. On the other hand, for mesoscale, time-varying events, the agreement is reasonable but the potential drops across the localized area may differ from those measured by the radar or satellite [Clauer et al., 1994; Emery et al., 1995; Papitashvili et al., 1995]. This can be caused by spatially localized ionospheric conductivity irregularities, especially during winter and equinox months when the UV-related conductivity is low. Comparisons with the IZMEM-predicted field-aligned currents (FAC) are still limited [Dremukhina et al., 1985; R. M. Winglee et al., Comparisons of the high-latitude ionospheric electrodynamics inferred from

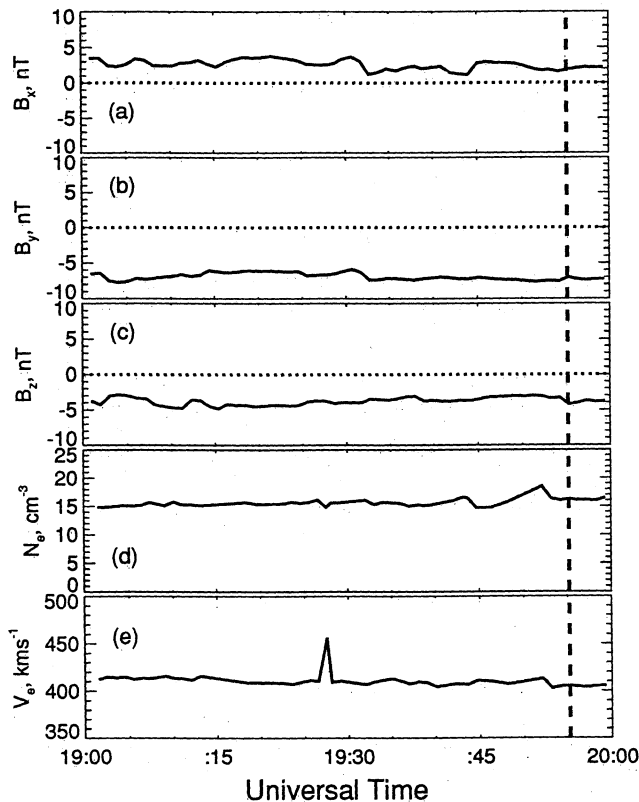


**Figure 1.** The IMF and solar wind data measured by the IMP 8 spacecraft on March 6, 1994. The vertical line at 1955 UT indicates a time instance for which the IZMEM model predictions were compared with the SuperDARN radar observations.

MHD and semiempirical models during the January 1992 GEM campaign, submitted to *Journal of Geophysical Research*, 1997].

Kustov *et al.* [1996] have undertaken an initial study of the IZMEM modeling performance by comparing the global model predictions of ionospheric electric fields with the locally averaged SuperDARN radar measurements on March 6, 1994 (1955 UT) during stable IMF conditions ( $B_z \approx B_y \approx -5$  nT). In this study we apply a "point-to-point" comparison between the IZMEM and SuperDARN data for the same event but extend a scope of the study adding three additional events for various IMF conditions.

The purpose of this study is now twofold. First, we compare two-dimensional ionospheric convection maps obtained from the Saskatoon-Kapuskasing pair of SuperDARN radars over the dayside high-latitude ionosphere with the corresponding patterns modeled from the IZMEM electric fields at altitudes where radar measurements take place ( $\sim 300$  km) for the southward and northward IMF conditions. Second, the analysis is extended by including the comparison between field-aligned currents inferred from the SuperDARN data [e.g., Sofko *et al.*, 1995] and corresponding FAC distributions modeled by IZMEM. These allow us to make some conclusions about the potential of SuperDARN to

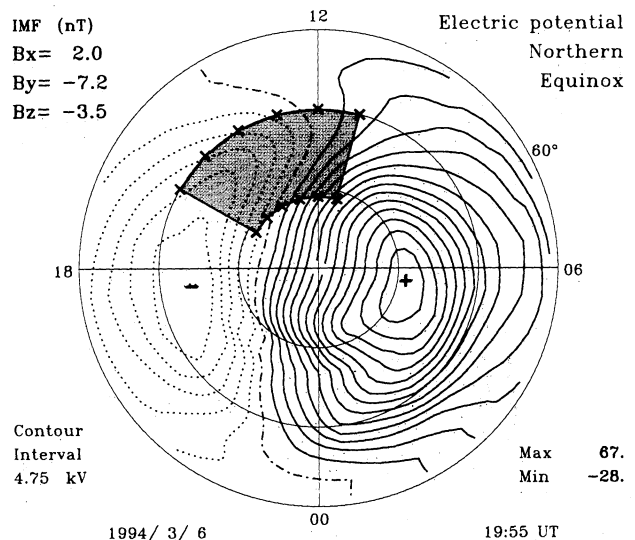
resolve the structure of global ionospheric convection and about the predictability of global convection patterns obtained solely from the IZMEM modeling when the IMF data are available.

## 2. Modeling and Observations During Quasi-Stable Southward IMF

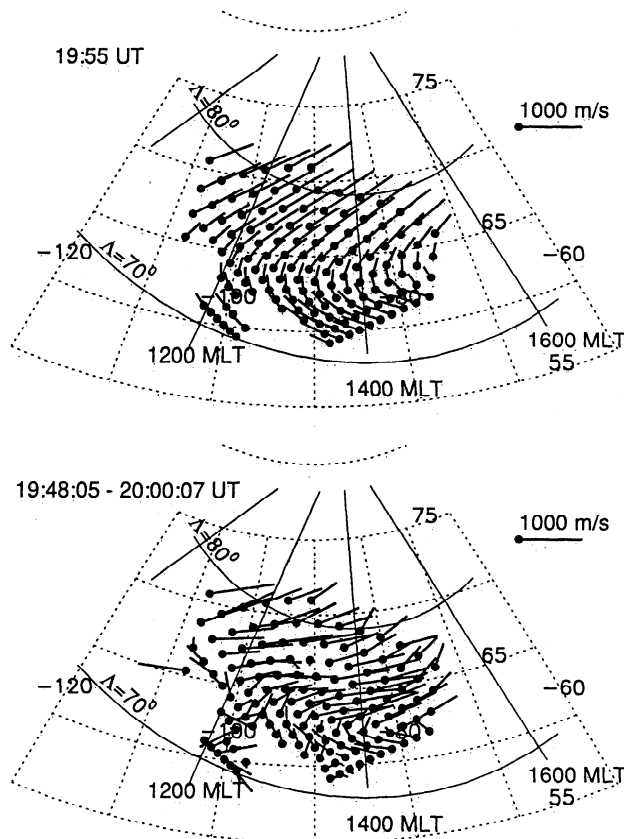
It is well established that for the southward IMF the global ionospheric convection is generally represented by the standard two-cell pattern with an antisunward flow across the center of the polar cap. To test the IZMEM performance for such a situation, the time interval 1900–2000 UT on March 6, 1994, was selected. During this event, the IMF was relatively stable and the radars observed echoes across a significant portion of the dayside ionosphere.

Figure 1 shows the IMP 8 solar wind plasma and IMF measurements for the selected interval; the time instance for comparison of the IZMEM predictions and radar measurements is marked by a vertical dashed line at 1955 UT. The IMP 8 spacecraft was located at this time in the solar wind at  $X_{GSM} = 14$ ,  $Y_{GSM} = 15$ , and  $Z_{GSM} = 31 R_E$ . During the previous hour the IMF  $B_z$  and  $B_y$  components were very stable; the solar wind velocity was about 410 km/s and density  $\sim 15$  cm $^{-3}$ . For the IZMEM modeling we utilized the average IMF values over 20 min prior to the radar measurements:  $B_z = -3.5$  nT and  $B_y = -7.2$  nT.

Figure 2 shows the electrostatic potential distribution as predicted by the IZMEM for 1955 UT. The highlighted area from 1100 to 1500 MLT shows the region covered by the Saskatoon-Kapuskasing Super-



**Figure 2.** The electrostatic potential distribution over the northern high-latitude ionosphere obtained from the IZMEM model for 1955 UT on March 6, 1994. The plus and minus signs mark locations of foci of the large-scale convection cells; the maximum and minimum values of electrostatic potential at these points are given at the bottom of the diagram.



**Figure 3.** Plasma convection vectors obtained from (top) the IZMEM model and from (bottom) the SuperDARN observations for 1955 UT on March 6, 1994.

DARN pair. The ionospheric convection is represented by the standard two-cell pattern with a slightly dominant dawn cell and elongated dusk cell in agreement with the negative  $B_y$  signature. The cross-polar cap potential drop is predicted to be  $\text{MAX} - \text{MIN} = 68 + 28 = 96$  kV.

Figure 3 shows a dayside portion of Figure 2 where the IZMEM convection is mapped in geographic coordinates and converted into the ion drift velocities (top) calculated at the collocated points where radars receive clear echoes (bottom). For IZMEM the velocity vectors were inferred from the modeled electric fields at altitude 300 km as  $\mathbf{V} = \mathbf{E} \times \mathbf{B}$ , where  $|\mathbf{B}|$  is the absolute value of the vertical component of the main geomagnetic field at these points obtained from the International Geomagnetic Reference Field (IGRF) model for Epoch 1994. One can see that both sets of velocity vectors exhibit the same pattern, namely, westward flow at the lower latitudes and eastward flow at the higher latitudes. Certainly, the model shows smoother flows but, in general, the prediction and measurements agree fairly well.

Comparing the “point-to-point” values, we see a few exceptions. At the lower latitudes, several points show that the predicted and measured velocity vectors are oriented in quite different directions. These points decrease significantly the correlation coefficients between

the two data sets to 0.45 and 0.42 for the magnitudes and for the vector azimuths, respectively. If we omit these points, then the correlation coefficients increase to 0.62 for the magnitudes and 0.74 for the azimuths. The latter numbers are closer to the results reported by *Kustov et al.* [1996], who compared the IZMEM predictions at the grid nodes with the closest SuperDARN vectors averaged around each node.

Note that the suggested omission of some “bad” points does not mean that we want “to cook” our statistics. The correlation between two patterns (even if they are almost identical in their configuration or shape) can be fairly small if these patterns are slightly shifted spatially against each other. However, for the event under investigation, the IZMEM and SuperDARN data show very similar convection patterns: for example, the convection reversal boundary is determined by the radars as well as by IZMEM along 1400 MLT at  $74.5^\circ$ , though the lower-latitude portion of the “radar” convection is inconsistent with the general pattern. A spot of reduced vectors (a quasi-vortex?) is observed by radars near 1300 MLT and  $77.5^\circ$ ; such a small-scale structure can be caused by a localized ionospheric irregularity. The latter may not be manifested as the gradient in the statistical ionospheric conductivity model; therefore it cannot be locally modeled by the IZMEM.

There is also no guarantee that radars measure “true” convection if some points show opposite or chaotically distributed vectors, comparing with the bulk of vectors on a map. We believe that if  $\sim 90\%$  of observed convection velocities are organized in a consistent global convection pattern, we can omit some “bad” measurements for a better comparison with the model. We show in Table 1 the difference between these two approaches.

In this study we shall characterize differences between predictions and measurements in the following way. For the magnitude, a fractional difference between two vectors  $\delta V_i$  is estimated at each individual point:

$$\delta V_i = \frac{|\vec{V}_{SD}^i| - |\vec{V}_{IZMEM}^i|}{|\vec{V}_{SD}^i|}$$

Here  $|\vec{V}_{SD}^i|$  and  $|\vec{V}_{IZMEM}^i|$  are the absolute values of the measured and predicted velocities at each point  $i$ . Then the absolute values of  $\delta V_i$  are averaged over the entire covered area (i.e., for all points available for the comparison within the individual SuperDARN convection map):

$$\Delta V_{av} = \frac{1}{n} \sum_{i=1}^n |\delta V_i|,$$

where  $n$  is the number of points within the map (typically more than 50).

For the vector azimuths the difference in azimuths  $\delta\theta_i$  at each point is defined as

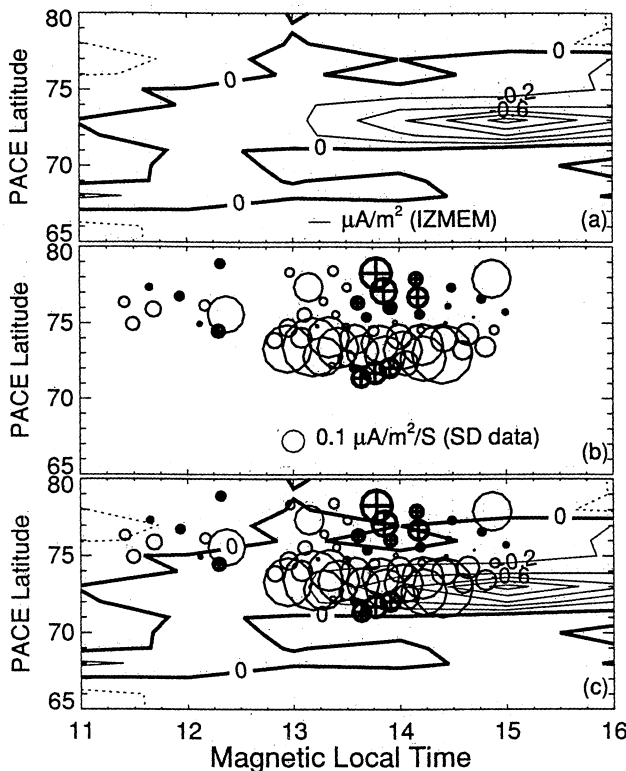
$$\delta\theta_i = \theta_{SD}^i - \theta_{IZMEM}^i$$

**Table 1.** Differences Between the Ion Drift Velocities Observed by SuperDARN Radars and Modeled by IZMEM

Date	UT	IMF, nT		All Points		No Opposite Points	
		$B_z$	$B_y$	$\Delta V_{av}$	$\Delta \theta_{av}^\circ$	$\Delta V_{av}$	$\Delta \theta_{av}^\circ$
March 6, 1994	1955	-3.5	-7.2	0.50	46	0.25	18
December 23, 1994	2030	+1.6	+4.1	0.62	31	0.55	19
December 23, 1994	2131	+1.7	-0.6	0.71	91		
January 10, 1994	1940	+4.0	+0.8	2.10	79		

where  $\theta_{SD}^i$  and  $\theta_{IZMEM}^i$  are the azimuths of the velocity vectors (measured and predicted, respectively). Then the absolute values of  $\delta\theta_i$  are averaged over the SuperDARN convection map area:

$$\Delta\theta_{av} = \frac{1}{n} \sum_{i=1}^n |\delta\theta_i|$$



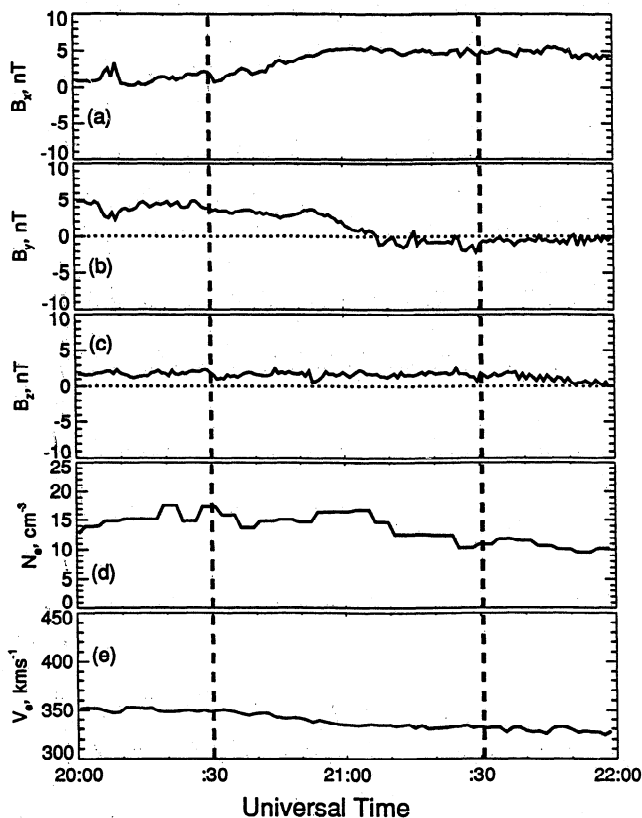
**Figure 4.** The IZMEM/SuperDARN field-aligned current comparison for 1955 UT on March 6, 1994: (a) the current distribution from IZMEM model (solid contours correspond to the upward currents; dashed contours correspond to the downward currents), (b) field-aligned currents inferred from SuperDARN observations by using the “curl-processing” technique (upward currents are denoted by the open circles; the downward currents are denoted by the circles with crosses; the size of each circle is proportional to the current’s intensity; the scale is shown at the bottom of this panel), and (c) both the IZMEM and SuperDARN FACs are plotted together. Note that the Polar Anglo-American Conjugate Experiment (PACE) coordinate system was introduced by Baker and Wing [1989] for the conjugate radar studies; this system is identical to the commonly used corrected geomagnetic coordinates. The PACE latitudes  $\lambda = 70^\circ$  and  $\lambda = 80^\circ$  are also shown in Figure 3.

Table 1 shows  $\Delta V_{av}$  and  $\Delta \theta_{av}^\circ$  for several events under investigation. First, all available points after the SuperDARN observations are included. One can see that in this case the differences between the model and observations are larger than 50% for the magnitudes and  $50^\circ$  for the azimuths. However, if  $\sim 10\%$  of points with almost opposite (predicted against measured) flow direction are omitted, the agreement between the SuperDARN data and the IZMEM model becomes much better. This clearly indicates that the IZMEM model can predict well the global convection pattern but not the local flow inhomogeneities obtained from radar measurements (which are still under question to be “true” or “false”). The differences in magnitude reduce to less than 50% for three events studied in this paper; the azimuth agreement becomes better than  $25^\circ$ . We conclude here that the SuperDARN convection maps and corresponding IZMEM modeling are in good agreement in a sense of representing the global convection pattern.

Another electrodynamic parameter which can be derived from the SuperDARN observations and then compared with the IZMEM predictions is the field-aligned current distribution. Recently, Sofko *et al.* [1995] developed the “curl-processing” technique for estimation of the FAC from direct SuperDARN observations assuming a uniformity of the ionospheric conductivity in the localized area.

Figure 4a shows the FAC distribution in the same MLT sector on March 6, 1994, obtained from the IZMEM modeling. The upward currents are shown by the solid contours, and the downward currents are shown by the dashed contours. Figure 4b shows the FAC distribution inferred from radar measurements where the FAC strength is presented per siemens of the height-integrated Pedersen conductivity (see details given by Sofko *et al.* [1995]). The upward currents are denoted by the open circles, the downward currents are denoted by the circles with pluses. The size (diameter) of each circle is proportional to the derived FAC intensity at each individual point of the radar map (a scale circle for  $0.1 \mu A/m^2/S$  is shown at the bottom of this panel).

One can see that locations of the predicted and measured field-aligned currents are generally in good agreement (Figure 4c, measured and predicted FACs are overlaid). For the upward currents in the region where the IZMEM and SuperDARN FACs are mainly overlaid, a typical FAC magnitude obtained from the IZMEM model is about  $0.3 \mu A/m^2$ . If we take the height-



**Figure 5.** The same as in Figure 1 but for 2030 and 2131 UT on December 23, 1994, Wind data.

integrated Pedersen conductivity in this region equal  $\sim 3$  S [e.g., Wallis and Budzinski, 1981], then the radar observations and the IZMEM modeling agree fairly well.

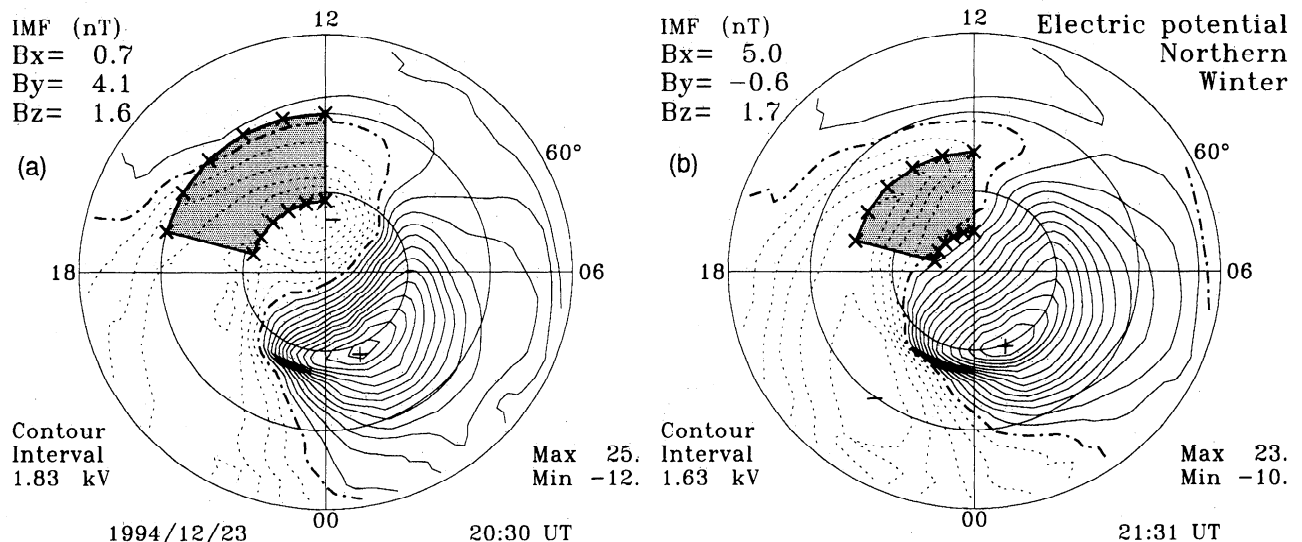
### 3. Modeling and Observations During Quasi-Stable Northward IMF

The plasma convection pattern and the distribution of field-aligned currents are much more complicated for northward IMF [e.g., Kamide and Baumjohann, 1993].

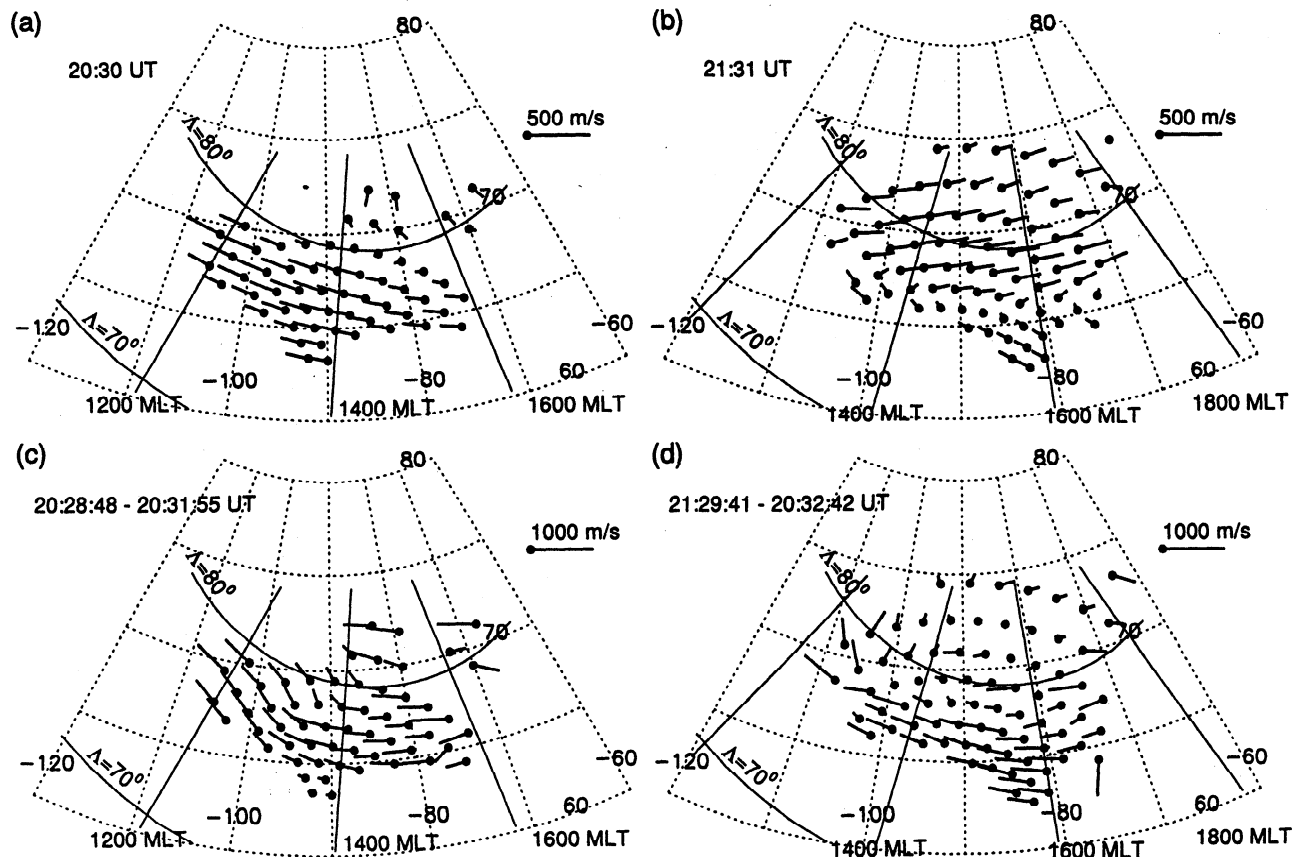
We compare radar observations with the IZMEM modeling for two situations:  $B_y$  is larger than  $B_z$  and  $B_z$  is larger than  $B_y$ . Figure 5 shows the Wind spacecraft measurements of the IMF and solar wind parameters on December 23, 1994, from 2000 to 2200 UT. The spacecraft was located at  $X_{\text{GSM}} = 23$ ,  $Y_{\text{GSM}} = -10$ , and  $Z_{\text{GSM}} = -3.4 R_E$ . The IMF was northward and stable, but the IMF  $B_y$  component decreased from 4 nT to small negative values. The solar wind plasma parameters were quite stable.

Figure 6 shows the electrostatic potential distribution as predicted by the IZMEM model for 2030 and 2131 UT. The radar observations cover the dayside sector from 1200 to 1700 MLT. In both cases a distorted two-cell convection pattern is developed which is typical for the winter season [e.g., Heppner and Maynard, 1987; Papitashvili et al., 1994]. A clear difference is seen in the dayside "throat" location, which depends on the IMF  $B_y$  direction.

For the first event the radar data are in a reasonable agreement with the IZMEM predictions as shown in Figure 7a for the collocated points. The second event shows a convection reversal boundary near  $76^\circ$  in the IZMEM pattern, but this reversal boundary is subtle in the SuperDARN data and can be located somewhere between  $79^\circ$  at 1300 MLT and  $82^\circ$  invariant latitude at 1600 MLT. According to the potential plot, the radar view area (highlighted on Figure 6b) covers the region with a ionospheric shear flow, that is, even the IZMEM's convection flow is sharply bent. Here we can only reveal a qualitative agreement between two patterns: both show the convection reversal boundaries but displaced by about  $5^\circ$ . Such a displacement can be related to improper selection of the IMF parameters for the modeling. Just a little reduction of the IMF azimuthal component ( $B_y = -0.1$  nT) shifts the IZMEM reversal boundary at higher latitudes ( $78^\circ$ ; one can model this via the Space Physics Research Laboratory Web site (<http://sprl.umich.edu/MIST>)).



**Figure 6.** The same as in Figure 2 but for (a) 2030 and (b) 2131 UT on December 23, 1994.



**Figure 7.** Plasma convection vectors obtained from (a,b) IZMEM model and (c,d) SuperDARN observations for 2030 UT and 2131 UT on December 23, 1994.

For this event we cannot omit “bad” points in our statistical analysis showing differences in the velocity magnitudes and vector azimuths and presented in Table 1. The IZMEM predictions of the FAC distributions in the radar “field-of-view” region are compared with experimental data in Figure 8. Here we also see reasonable agreement for the first event but the upward currents are not colocated for the second event because the reversal boundaries are significantly different.

The studied events (Figures 1–8) were relatively simple cases for which either the southward  $B_z$  or the  $B_y$  component dominated. As a more complicated situation, we selected the event of January 10, 1994, extensively studied by *Greenwald et al.* [1995b]. The authors concluded that on this day the SuperDARN radars observed the postnoon convection vortex related to the strong northward IMF and caused by the northward  $B_z$  (NBZ) field-aligned current system [*Iijima et al.*, 1984].

Figure 9 shows the IZMEM electrostatic potential distribution which clearly depicts the reverse convection near noon and both NBZ-generated reverse convection cells; the global picture can be interpreted either as a distorted two-cell convection pattern or a multicell convection. In this example, both the prenoon and postnoon reverse convection cells are well developed on the background of a standard two-cell convection pattern related to the quasi-viscous interaction between the solar wind plasma and Earth’s magnetosphere.

Figure 10 shows the IZMEM modeling of ionospheric convection in the collocated points with the SuperDARN observations. One can see that qualitatively the IZMEM model exhibits a vortex which is very similar to the observed one. There are eastward and westward flows at latitudes  $\Lambda = 77^\circ - 80^\circ$  and  $\Lambda = 82^\circ - 85^\circ$ , respectively. Corresponding reversals from the eastward flow to the westward flow and vice versa occur near 1200 and 1500 MLT meridians. Obviously, the magnitudes of modeled and observed velocity vectors are different, especially in the regions of flow reversals. One can also notice that the vortex focus is slightly shifted ( $\sim 5^\circ$  by the longitude) in the modeled pattern toward 1500 MLT against the SuperDARN observations. Spatially, the observed vortex is larger than the modeled one: its extension to the higher latitudes shows some opposite vectors against the model. Average differences between the model and observations are more than 200% in magnitudes and  $79^\circ$  in azimuths (Table 1); this is significantly larger than for the quasi-stable IMF events.

Though some differences between the IZMEM and experimental data have been reported earlier [e.g., *Feldstein et al.*, 1996], we can argue that for the event under investigation the IMF changes rapidly; therefore more detailed comparisons with better time resolution are required. One can see that the IZMEM model represents the convection pattern observed by radars reasonably well but it is a challenging task to select a proper time

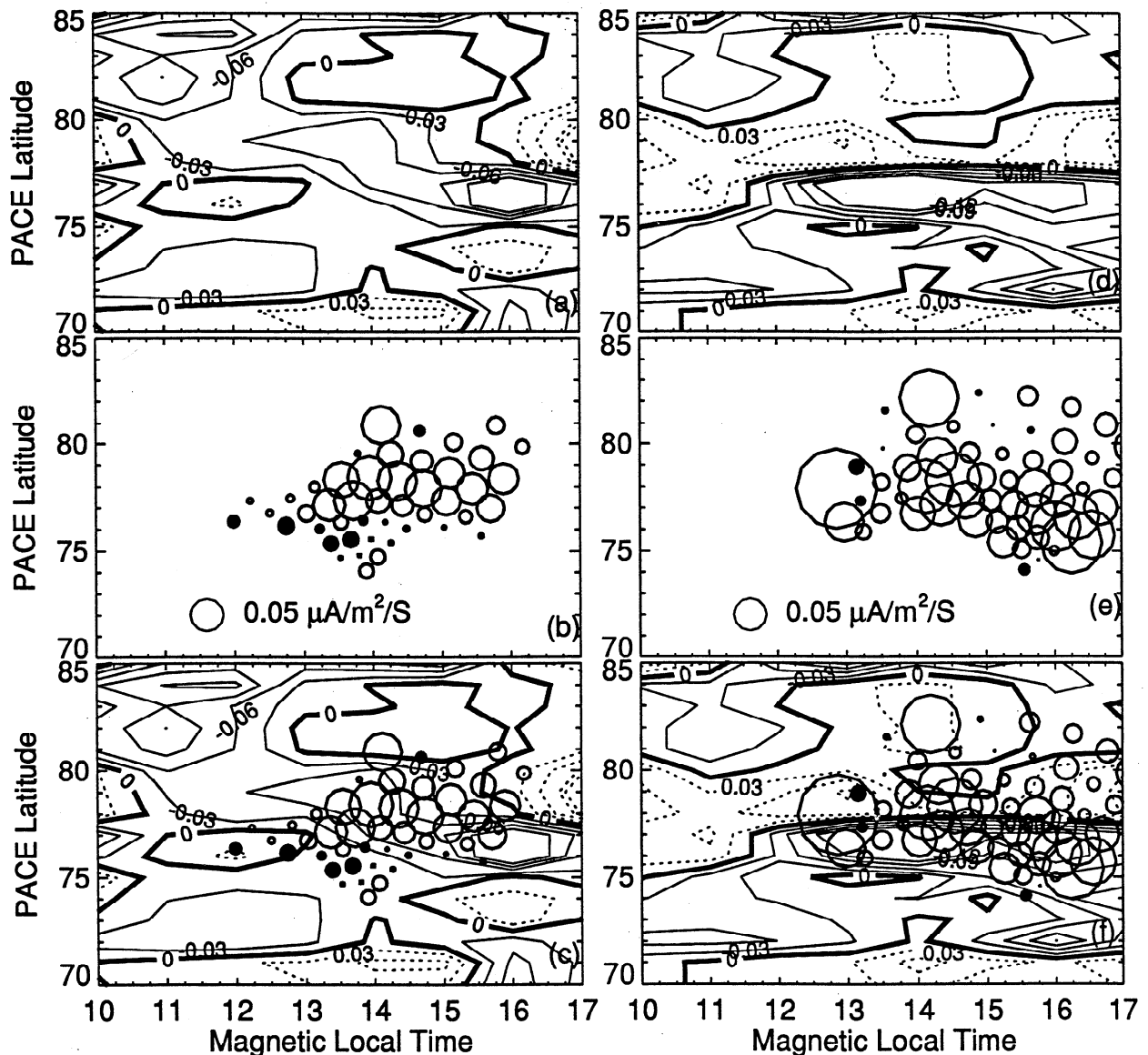


**Figure 8.** The same as in Figure 4 but for (left) 2030 UT and (right) 2131 UT on December 23, 1994.

delay and IMF values for the modeling. The radar data have been averaged over 30 min from 1925 UT in the original paper by *Greenwald et al.* [1995b] because for the shorter time-averaging intervals the radar echoes are patchy and can be inconclusive. Therefore the IMF data were also averaged over 30 min from 1915 UT when the  $B_y$  component dropped from 5 to about 1 nT, but  $B_z$  was still maintained at about 4 nT level. We remind the reader that this averaging is absolutely unrelated to the model construction timescale; the obtained IMF values are used for the ionospheric convection modeling within the “black box” approach (see details given by *Papitashvili et al.* [1994, 1995]).

Because of the above mentioned circumstances, the omission of oppositely directed vectors for the model/observation comparisons does not make sense, so we do not show the “omission” results in Table 1. Nevertheless, we think that this event provides a solid confirmation that the SuperDARN radars are able to determine the mesoscale dayside vortices related to the NBZ FAC cur-

rent system; these vortices are also clearly depicted by the IZMEM potentials (Figure 9). The recent study by *Greenwald et al.* [1996] provides more examples of the radar mesoscale vortex observations.

#### 4. Discussion and Conclusions

Comparisons with satellite and incoherent scatter radar measurements have shown that the IZMEM model can successfully predict a general configuration of the ionospheric convection pattern, location of the convection cell foci, and the MLT location of the flow reversals [*Dremukhina et al.*, 1985; *Feldstein and Levitin*, 1986; *Feldstein et al.*, 1994; 1996; *Papitashvili et al.*, 1989, 1995; *Ridley and Papitashvili*, submitted manuscript, 1997]. In this paper the first attempt is made to evaluate differences between the modeled patterns and the SuperDARN radar observations in a more quantitative fashion. For the events studied, the differences between



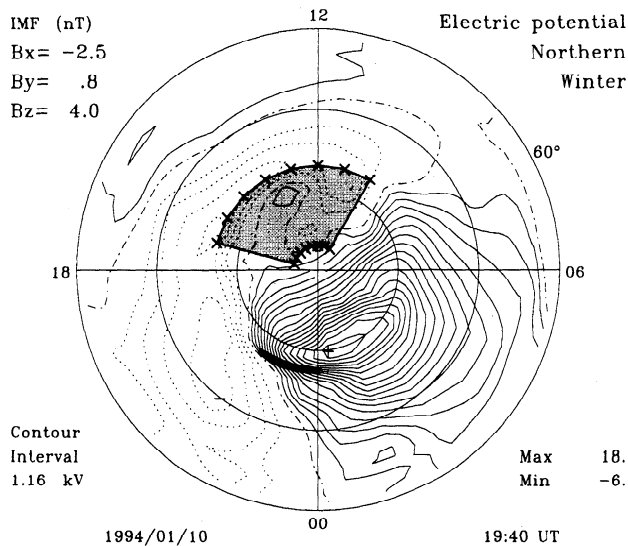


**Figure 9.** The same as in Figure 2 but for 1940 UT on January 10, 1994.

the predictions and measurements are found to be about 50% for the ion velocity magnitudes and  $\sim 25^\circ$  for the vector azimuths. This indicates that the IZMEM predictions are reasonable for representing the smoothed large-scale ionospheric convection patterns under the conditions of quasi-stable IMF. It also confirms that the calibration factors suggested for the IZMEM model by *Papitashvili et al.* [1994] are correctly defined.

One can make several remarks with respect to some differences between the model predictions and actual radar observations found in this study. We distinguish two types of differences. The first one comes from the small-scale, local irregularities when radars observe an appearance of the "convection isles" with totally different direction and/or magnitude of the ion velocity vectors with respect to the averaged, smoothed over the radar "field-of-view" pattern. We believe that in this case the radars lose steady echoes which appears as errors in the radar measurements. The possibility of such localized errors in the radar measurements have been reported earlier [e.g., *Villain et al.*, 1986].

Several effects might cause this. One is an occurrence of the double-peaked spectra due to the small-scale vortical flow within the radar scattering volume. This effect is especially significant when a large-scale shear flow is developed within the radars "field-of-view" [A. Schiffler et al., Mapping the outer low-latitude boundary layer with SuperDARN double-peaked spectra, submitted to *Geophysical Research Letters*, 1997]. Another effect is the ionospheric refraction which causes a lateral radio wave deviation from an assumed direction of the wave propagation. To take both of these effects into account, a detailed analysis of the SuperDARN data and supportive observations of ionospheric conditions must be performed for each individual radar observation.

For the events under investigation, no auxiliary measurements were available to scrutinize the SuperDARN data. We note that such a work is a current subject for

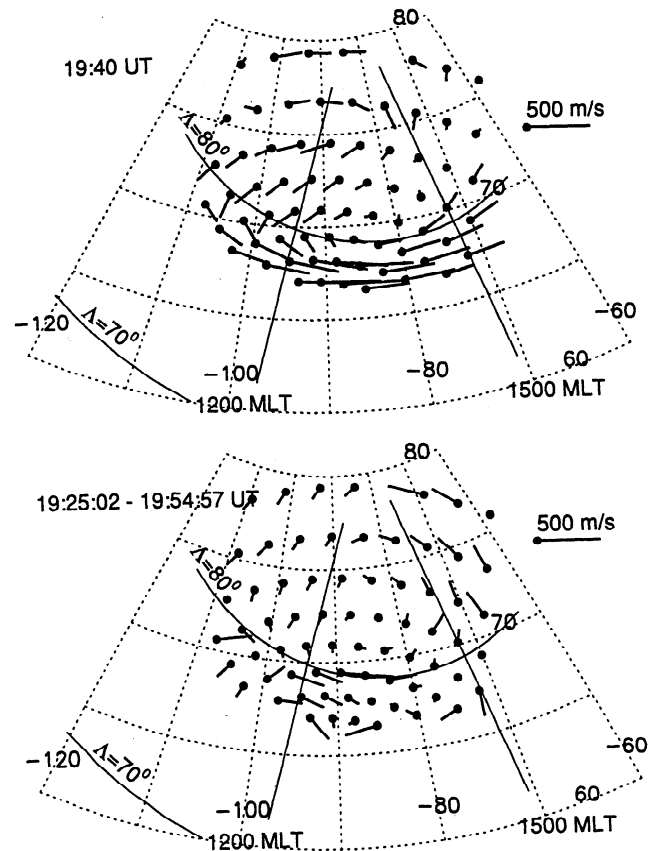


**Figure 10.** The same as in Figure 3 but for 1940 UT on January 10, 1994.

specific studies carried out by the SuperDARN community. We should say that in any case the routine SuperDARN maps represent a sort of "model" of the "true" convection pattern under observations since certain integration time and spatial averaging are applied. Therefore elimination of some points with an "abnormal" behavior within each "radar" convection map (i.e., points with the opposite vectors due to the radar observation errors) allows for a better comparison between the radar data and model predictions.

A second type of difference is a large-scale discrepancy in the observed and modeled patterns. This discrepancy is mainly originated from the spatial shift between the observed and modeled patterns. IZMEM has been developed as a technique to model large-scale, quasi-steady convection patterns with the aim to understand global structural elements of the magnetosphere-ionosphere coupling. After the model construction it was recognized that IZMEM is able to model surprisingly well the time-varying phenomena in the absence of substorms; however, the properly determined propagation time for the IMF changes measured by a spacecraft is required to identify the corresponding ionospheric manifestations [*Papitashvili et al.*, 1995; *Ridley and Papitashvili*, submitted manuscript, 1997]. For example, *Feldstein et al.* [1996] applied the IZMEM technique for studies of the ionospheric convection under the condition of time-varying IMF. The authors found that if one can make an appropriate choice of the time delay

between the IMF measurements by the IMP 8 spacecraft and the convection observations in the ionosphere, the IZMEM model provides reasonable estimates of the electric fields along the VIKING satellite trajectory. However, for some parts of the trajectory, especially in the morning sector, the modeled and observed values differ by a factor of 2 in magnitudes. This is in agreement with the conclusions of present study for the January 10, 1994, event. These studies show that there are some possibilities for a further improvement of the IZMEM model.

As for the field-aligned current distributions, the technique used by *Sofko et al.* [1995] is able to calculate only the "magnetospheric component" of the field-aligned currents, but their "ionospheric component" (due to the ionospheric conductivity gradients) is still unpredictable from the radar measurements. The authors assumed a scale size of conductivity gradients larger than 1000 km so that the "ionospheric component" was small within the SuperDARN convection variation scale (typically several hundred kilometers). This assumption is true for the summer, but considered events in the cited paper are from winter and equinox seasons; in this case conductivity gradients can be comparable with the radar "field-of-view" area and "ionospheric" contribution can be large enough to produce local irregularities.

The IZMEM model utilizes the nonuniform ionospheric conductivity model by *Wallis and Budzinski* [1981]. Therefore the IZMEM-modeled FACs contain both the "magnetospheric" and "ionospheric" components. The latter depends on the scale size provided by the conductivity model but does not fully consider small-scale ionospheric structures. Thus we think that at this stage and for the considered events the field-aligned currents obtained from SuperDARN data and modeled by IZMEM can only be compared qualitatively.

We conclude that the SuperDARN radars provide solid experimental confirmation for the convection structural elements obtained from IZMEM and other modeling techniques. Despite the fact that almost all above mentioned convection models have been obtained from experimental data (ground magnetometers or satellite observations), the complicated modeling algorithm and properly defined boundary conditions are required for the data inversion. The magnetometer-based models provide good global coverage but require the ionospheric conductivity models. The satellite-based observations (electric fields or ion driftmeter data) require accurate integration of experimental data along the satellite orbit and follow-on correction for the corotation potential; then some sort of expansion technique (Fourier or spherical harmonic analyses) is required for extension to a global coverage.

These are not the problems for the SuperDARN observations: the radar network covers almost the entire polar region, provides overlapping measurements from which the two-dimensional (2-D) convection patterns

can be easily inferred, and it does not involve any modeling algorithm to produce individual maps (except of a specific data processing technique for conversion of the "line-of-sight" ion velocities to the 2-D plasma drift maps). These are the chief advantages of the SuperDARN observations, though the global modeling of the convection patterns requires statistical averaging and a mathematical expansion of experimental data to fill the gaps in the HF radar observations [e.g., *Ruohoniemi and Greenwald*, 1996].

As shown by all events analyzed here, the comparison of SuperDARN observations and IZMEM modeling provides the good global context within which the radar observations can be better interpreted. On the other hand, localized real-time SuperDARN observations made by one or more pairs of radars can be utilized to adjust the global convection modeled by IZMEM solely from the IMF data through the spherical harmonic expansion procedure (in a manner as the AMIE technique incorporates the radar and satellite data to adjust in situ the global potential pattern obtained initially only from collected ground magnetometer data). This may provide a near-realistic specification of the global ionospheric convection for the space weather purposes. It is obvious that all available ionospheric convection models require extensive intercalibration and verification for further utilization in the practical applications.

**Acknowledgments.** The Kapuskasing HF radar was funded by the NASA grant NAG 5-1099. The Saskatoon HF radar is funded by the Canadian Natural Sciences and Engineering Research Council (NSERC) under a Collaborative Special Project Grant. Funding for this study was also provided by the NSERC operating grants (G.J.S. and A.V.K.) as well as by the Canadian Space Agency grant (A.V.K.). In Michigan the research was supported by the NSF grants OPP-9318766 and ATM-9523329 (V.O.P). In Russia the study was supported by grants 96-05-66279 and 96-05-65067 from the Russian Foundation for Fundamental Research and grant INTAS-RFBR-95-0932. The IMF data were obtained from the NASA National Space Science Data Center.

The Editor thanks N. C. Maynard and A. K. Pellinen-Wannberg for their assistance in evaluating this paper.

## References

- Baker, K. B., and S. Wing, A new magnetic coordinate system for conjugate studies at high latitudes, *J. Geophys. Res.*, **94**, 9139, 1989.
- Clauer, C. R., V. O. Papitashvili, A. J. Ridley, F. J. Rich, B. A. Belov, and A. E. Levitin, Comparison of the Sondrestrom radar and DMSP ion convection velocity measurements with the global electric field modeling, *Eos Trans. AGU*, **75**(16), Spring Meet. Suppl., 319, 1994.
- Dremukhina, L. A., Y. I. Feldstein, and A. E. Levitin, Model calculations of currents and magnetic fields along a Magsat trajectory, *J. Geophys. Res.*, **90**, 6657, 1985.
- Emery, B. A., W. F. Godesorkhi, A. D. Richmond, V. O. Papitashvili, C. R. Clauer, D. J. Knipp, B. A. Belov, and A. E. Levitin, Using and comparing IZMEM electric potentials with AMIE for the large magnetic cloud passage of January 14, 1988, paper presented at IUGG XXI General

- Assembly, Int. Union Geod. Geophys., Boulder, Colo., July 2-14, 1995.
- Feldstein, Y. I., and A. E. Levitin, Solar wind control of electric fields and currents in the ionosphere, *J. Geomag. Geoelectr.*, **38**, 1143, 1986.
- Feldstein, Y. I., A. E. Levitin, L. I. Gromova, L. A. Dremukhina, L. G. Blomberg, P.-A. Lindqvist, and G. T. Marklund, Electromagnetic weather at 100 km altitude on 3 August, 1986, *Geophys. Res. Lett.*, **21**, 2095, 1994.
- Feldstein, Y. I., L. I. Gromova, A. E. Levitin, L. G. Blomberg, G. T. Marklund, and P.-A. Lindqvist, Electromagnetic characteristics of the high-latitude ionosphere during the various phases of magnetic substorms, *J. Geophys. Res.*, **101**, 19,921, 1996.
- Foster, J. C., An empirical electric field model derived from Chatanika radar data, *J. Geophys. Res.*, **88**, 981, 1983.
- Friis-Christensen, E., Y. Kamide, A. D. Richmond, and S. Matsushita, Interplanetary magnetic field control of high-latitude electric field and currents determined from Greenland magnetometer data, *J. Geophys. Res.*, **90**, 1325, 1985.
- Greenwald, R. A. et al., DARN/SuperDARN: A global view of the dynamics of high-latitude convection, *Space Sci. Rev.*, **71**, 761, 1995a.
- Greenwald, R. A., W. A. Bristow, G. J. Sofko, C. Senior, and R. P. Lepping, SuperDARN radar imaging of dayside high-latitude convection under northward IMF: Towards resolving the distorted two-cell versus multicell controversy, *J. Geophys. Res.*, **100**, 19,661, 1995b.
- Greenwald, R. A., J. M. Ruohoniemi, W. A. Bristow, G. J. Sofko, J.-P. Villain, A. Huuskonen, S. Kokubun, and L. A. Frank, Mesoscale dayside convection vortices and their relation to substorm phase, *J. Geophys. Res.*, **101**, 21,697, 1996.
- Hairston, M. R., and R. A. Heelis, Model of high-latitude ionospheric convection pattern during southward interplanetary magnetic field using DE 2 data, *J. Geophys. Res.*, **95**, 2333, 1990.
- Heppner, J. P., and N. C. Maynard, Empirical high-latitude electric field models, *J. Geophys. Res.*, **92**, 4467, 1987.
- Iijima, T., T. A. Potemra, L. J. Zanetti, and P. F. Bythrow, Large-scale Birkeland currents in the dayside polar region during strongly northward IMF: A new Birkeland current system, *J. Geophys. Res.*, **89**, 7441, 1984.
- Kamide, Y., and W. Baumjohann, *Magnetosphere-Ionosphere Coupling*, Springer-Verlag, New York, 1993.
- Kamide, Y., A. D. Richmond, and S. Matsushita, Estimation of ionospheric electric fields, ionospheric currents and field-aligned currents from ground magnetic records, *J. Geophys. Res.*, **86**, 801, 1981.
- Knipp, D. J. et al., Ionospheric convection response to slow, strong variations in a northward interplanetary magnetic field: A case study for January 14, 1988, *J. Geophys. Res.*, **98**, 19,273, 1993.
- Kustov, A. V., G. J. Sofko, Y. I. Feldstein, L. I. Gromova, A. E. Levitin, R. A. Greenwald, and M. J. Ruohoniemi, Dayside convection: First results of the comparison between SuperDARN radar measurements and IZMEM model, *Geomagn. Aeron.*, **36** (5), 26, 1996.
- Levitin, A. E., R. G. Afonina, B. A. Belov, and Y. I. Feldstein, Geomagnetic variations and field-aligned currents at northern high-latitudes and their relations to solar wind parameters, *Philos. Trans. R. Soc. London Ser., A*, **304**, 253, 1982.
- Maynard, N., Space weather prediction, *U.S. Natl. Rep. Int. Union Geod. Geophys. 1991-1994, Rev. Geophys.*, **33**, 547, 1995.
- Papitashvili, V. O., and N. E. Papitashvili, Cross-polar electric potentials and AE index, in *The Evaluation of Space Weather Forecasts: Proceedings of a Workshop at Boulder, Colorado, June 19-21, 1996*, edited by K. Doggett, pp. 39-50, NOAA/Space Environment Center, Boulder, Colo., 1996.
- Papitashvili, V. O., B. A. Belov, and L. I. Gromova, Field-aligned currents and convection patterns in the southern polar cap during stable northward, southward, and azimuthal IMF, *IEEE Trans. Plasma Sci.*, **17**(2), 167, 1989.
- Papitashvili, V. O., Y. I. Feldstein, A. E. Levitin, B. A. Belov, L. I. Gromova, and T. E. Valchuk, Equivalent ionospheric currents above Antarctica during the austral summer, *Antarct. Sci.*, **2**, 67, 1990.
- Papitashvili, V. O., B. A. Belov, D. S. Faermark, Y. I. Feldstein, S. A. Golyshev, L. I. Gromova, and A. E. Levitin, Electric potential patterns in the northern and southern polar regions parameterized by the interplanetary magnetic field, *J. Geophys. Res.*, **99**, 13,251, 1994.
- Papitashvili, V. O., C. R. Clauer, A. E. Levitin, and B. A. Belov, Relationship between the observed and modeled modulation of the dayside ionospheric convection by the IMF  $B_y$  component, *J. Geophys. Res.*, **100**, 7715, 1995.
- Rich, F. J., and M. Hairston, Large-scale convection patterns observed by DMSP, *J. Geophys. Res.*, **99**, 3827, 1994.
- Richmond, A. D., Assimilative mapping of ionospheric electrodynamics, *Adv. Space Res.*, **12** (6), 59, 1992.
- Richmond, A. D., and Y. Kamide, Mapping electrodynamic features of the high-latitude ionosphere from localized observations: Technique, *J. Geophys. Res.*, **93**, 5741, 1988.
- Ruohoniemi, J. M., and R. A. Greenwald, Statistical patterns of high-latitude convection obtained from Goose Bay HF radar observations, *J. Geophys. Res.*, **101**, 21,743, 1996.
- Sofko, G. J., R. Greenwald, and W. Bristow, Direct determination of large-scale magnetospheric field-aligned currents with SuperDARN, *Geophys. Res. Lett.*, **22**, 2041, 1995.
- Villain, J.-P., C. Beghin, and C. Hanuise, ARCAD-SAFARI coordinate study of auroral and polar  $F$ -region ionospheric irregularities, *Ann. Geophys.*, **4**, 61, 1986.
- Wallis, D. D., and E. E. Budzinski, Empirical models of height-integrated conductivities, *J. Geophys. Res.*, **86**, 125, 1981.
- Weimer, D. R., Models of high-latitude electric potentials derived with a least error fit of spherical harmonic coefficients, *J. Geophys. Res.*, **100**, 19,595, 1995.
- Weimer, D. R., A flexible, IMF dependent model of high-latitude electric potentials having "space weather" applications, *Geophys. Res. Lett.*, **23**, 2549, 1996.
- B. A. Belov, Ya. I. Feldstein, L. I. Gromova, and A. E. Levitin, Institute of Terrestrial Magnetism, Ionosphere, and Radio Wave Propagation, Troitsk, 142092, Russia. (e-mail: bbelov@adonis.iasnet.com; sgc@node.ias.msk.su; gromova@izmiran.rssi.ru)
- R. A. Greenwald and M. J. Ruohoniemi, Applied Physics Laboratory, Shipping Receiving Facility, 11100 Johns Hopkins Rd., Laurel, MD 20723. (e-mail: ray-greenwald@jhuapl.edu; mike.ruohoniemi@jhuapl.edu)
- A. V. Kustov, A. Schiffler, and G. J. Sofko, Institute of Space and Atmospheric Studies, University of Saskatchewan, Physics Building, 116 Science Place, Saskatoon, SK, Canada S7N 5E2. (e-mail: kustov@dansas.usask.ca; andreas@karlsberg.usask.ca; sofko@dansas.usask.ca)
- V. O. Papitashvili, Space Physics Research Laboratory, University of Michigan, 2455 Hayward, Ann Arbor, MI 48109. (e-mail: papita@pitts.sprl.umich.edu)

(Received February 5, 1997; revised July 21, 1997; accepted August 6, 1997.)